Open Access Journal
Journal of Power Technologies 94 (Nuclear Issue) (2014) 77–84
journal homepage:papers.itc.pw.edu.pl

Development of a measurement and reconstruction system for determining the phase distribution in a two-phase flow vertical tube using Electrical Impedance Tomography

Michał Gatkowski*,[a], Thomas Buchner[b], Grzegorz Niewiński[a], Piotr Mazgaj[a]

[a]*Institute of Heat Engineering, Warsaw University of Technology*
21/25 Nowowiejska Street, 00-665 Warsaw, Poland
[b]*Avera NP GmbH, Erlangen, Gernmany*

Abstract

This paper is based on experience gained during six months of work on Electrical Impedance Tomography (EIT) at the Areva NP test facility in Erlangen, Germany. The aim of this work was to build an EIT system capable of providing fairly accurate imaging of the resistivity field in a vertical pipe with two-phase flow. The described system will be used to analyze two-phase flow in the PKL Integral Test Facility. EIT is an imaging method in which electrical current is injected through electrodes into a volume of interest and the potential distribution obtained is measured by surface electrodes. Using these measurements an image of the electrical conductivity/resistivity can be reconstructed in the volume of interest using numerical techniques. The reconstruction is difficult because the mathematical problem is ill-posed and non-linear, which implicates high computational intensiveness.

Keywords: Electrical Impedance Tomography, Two-phase flow, Phase distribution measurement, Nuclear I&C

1. Introduction

Measurement of the local phase distribution is hard to define due to operating conditions with invasive fluids or high thermal parameters. Optical methods are difficult or impossible to implement. Therefore, for this measurement task it is better to place the sensors on the periphery of the evaporator tube. In geophysics relatively simple and cost-effective tomographic methods are being used. Design is based on Electrical Impedance Tomography (EIT). In this paper a measurement system for the determination of phase distribution in a suitable water-air flow channel under ambient conditions will be developed. This system is intended to form a basis for the possible evolution of the system for industrial application under operational conditions of steam power plants (in particular, nuclear power plants) with the aim being to obtain suitable boundary conditions for numerical flow calculations. In this case the determination of the phase distribution is performed with electrodes installed evenly on the pipe periphery and using the electric field produced by them in the flow. The local field strength of this electric field is the conductivity distribution and thus is determined by the phase distribution of the flow, due to differences in water and steam conductivity.

*Corresponding author
Email address: mueenmalik9516@gmail.com (Michał Gatkowski*,)

Electrical process tomography, including electrical capacitance tomography (ECT), electrical impedance tomography (EIT) and electromagnetic tomography (EMT), is based on the specific properties of materials principally sensed by each technique.
In the case of EIT, the sensor is made from multiple electrodes arranged around the periphery of the internal wall of the process vessel or pipeline, in contact with the process medium. A current is applied to some electrodes and voltages are measured from the other electrodes, according to a predefined strategy. Then these voltage measurements are used to reconstruct the impedance distribution inside the vessel with a specific inverse algorithm.
This system is developed in order to install it in the PKL Integral Test Facility (a downsized nuclear reactor facility that is used to simulate the complex processes in pressurized water reactors (PWRs)), in order to study two-phase flows during accidents.

2. Theory

The basis of electrical tomography or electrical impedance tomography (EIT) is the detection and exploitation of differing electrical properties (capacitance, resistance, induction) of the material or materials under investigation within the imaging volume. Based on these properties, electrical measurements from numerous points around a vessel or pipeline are utilized. An array of spaced electrodes, often arranged in a plane, are fixed to the boundary wall of a vessel to map the changing spatial distribution of resistivity (or its inverse, conductivity) of the material contained within. The resulting signals are interpreted by a computer and the resulting boundary datasets, inverted by means of an image reconstruction technique to provide a distribution map of the internal resistivity/permittivity, are used to create a series of 2D or 3D images of the process occurring within [1].

2.1. Physical model

The electromagnetic field within a body Ω is governed by the Maxwell Equations.

$$\nabla \times E = -\frac{\partial B}{\partial t} \tag{1}$$

$$\nabla \times H = J + \frac{\partial D}{\partial t} \tag{2}$$

The electric displacement D and the magnetic induction B can be expressed in terms of the electric field E and the magnetic field H as:

$$D = \epsilon E \tag{3}$$

$$B = \mu H \tag{4}$$

Where ϵ and μ denote the electrical permittivity and magnetic permeability respectively. At this stage, we follow the assumption of isotropic ϵ, μ and electric conductivity σ and leave the anisotropic case for other studies. Substituting the current density as $J = \sigma E$ and applying the plane-wave definitions for the electric field, $E = \hat{E}e^{i\omega t}$, and the magnetic field $B = \hat{B}e^{i\omega t}$, equations (1) and (2) can be rewritten into the form:

$$\nabla \times E = -i\omega\mu H \tag{5}$$

$$\nabla \times H = J + i\omega\epsilon E \tag{6}$$

The two components forming $J = J_0 + J_S$ are the current density caused by ohmic current $J_0 = \sigma E$, and the current density resulting internal sources, J_S, can be neglected. Thus we obtain the Maxwell Equations applicable to EIT in the form:

$$\nabla \times E = -i\omega\mu H \tag{7}$$

$$\nabla \times H = (\sigma + i\omega\epsilon)E \tag{8}$$

To simplify the calculations we neglect the electric field contributed by magnetic induction and hence we use the definition of E under quasi-static conditions,

$$E = -\nabla\phi \tag{9}$$

where ϕ is the electric potential. Substituting equation (9) into equation (6) and taking the divergence of both sides yields

$$\nabla \cdot (\nabla \times H) = \nabla \cdot (\sigma + i\omega\epsilon)E \tag{10}$$

$$0 = \nabla \cdot (\sigma + i\omega\epsilon)\nabla\phi \tag{11}$$

Hence the governing equation for Electrical Impedance Tomography inside body Ω becomes

$$\nabla \cdot (\sigma + i\omega\epsilon)\nabla\phi = 0 \tag{12}$$

Applying low frequency or direct currents reduces equation (12) to the governing equation for Electrical Resistance Tomography (ERT), which is often referred to as the governing equation for EIT:

$$\nabla \cdot (\sigma\nabla\phi) = 0 \tag{13}$$

The approximation is valid as long as ω is within a range of approximately 0–42 kHz in which the capacitive properties of water and some dielectric materials may vary [2].

2.2. *Electrode models and boundary condition*

Equation (13) is a second order elliptic partial differential equation (PDE) in ϕ. To exist as a unique solution, the definition of the boundary condition (BC) is required. The BCs for this PDE depend on the electrode type (material properties) and the model assumed for its behavior.

Continuum model. The continuum model, which does not take into account the presence of electrodes, is the simplest case of BCs. The current density j applied in normal inward direction N to the object's surface, $\partial\Omega$, is then defined as:

$$j = \sigma\frac{\partial\phi}{\partial n} \text{ on } \partial\Omega \tag{14}$$

The gap model. Though the alternative gap model does account for the presence of N_L electrodes and assumes the injection of current I_l into electrode number l with area S_l,

$$j = \frac{I_l}{S_l} \quad l = 1, 2...N_L \tag{15}$$

$$j = 0 \quad \text{in gaps between electrodes} \tag{16}$$

it is much more accurate than the continuum model.

3. Simulation

The simulation of the test setup and reconstruction of images was done by EIDORS (Electrical Impedance and Diffuse Optical Tomography Reconstruction Software). EIDORS is an open source suite code for image reconstruction in electrical impedance tomography (EIT). One goal of this code is to provide freely distributable and modifiable software for image reconstruction of electrical data. EIDORS is run by the Matlab package and has portable modular architecture, open-source licensing, and enhanced finite element modeling.
Initial simulations were conducted with 8 electrodes. The main reason for that was to calculate older experimental data (this data was harvested with an earlier experimental setup) with the new code. This comparison showed the results to be very similar. Reconstruction with simulated data gave some feedback about electrode voltage switching patterns. Then the simulation was changed to 16 electrodes, to develop better resolution in the flow channel [3].

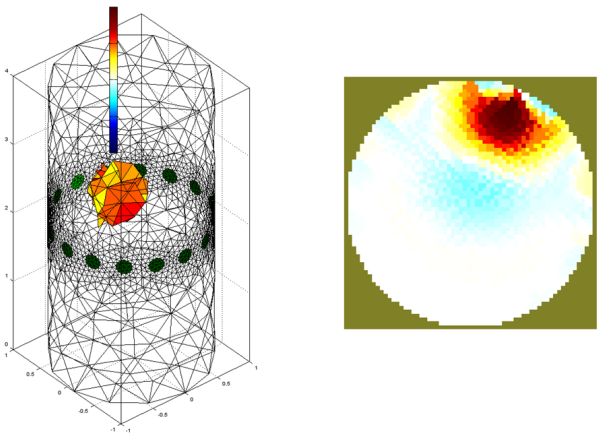

Figure 1: Left: 3D mesh with high resistivity inclusion (radius 0.2) represents real experiment situation. Right: reconstruction of 3D forward data on 2D planar mesh, representation of experiment reconstruction situation

Overall knowledge gained after a series of comparison simulations was promising for adjacent stimulation and mono measurement. With high density meshes the accuracy in reconstruction of the position of inclusion is much more precise, in low density meshes this effect is less visible. Images from

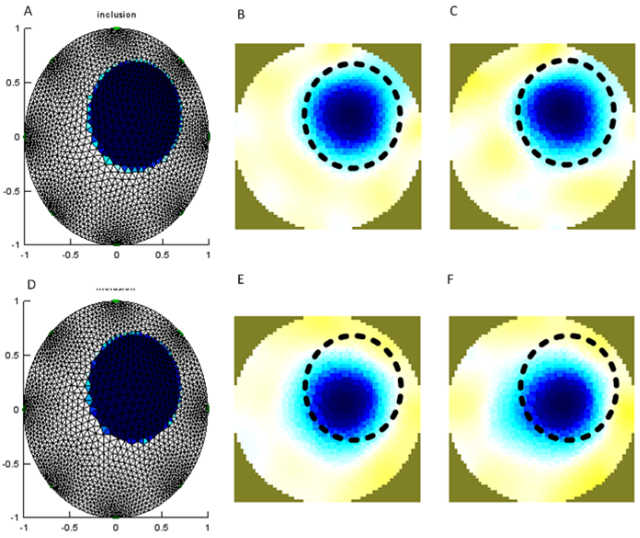

Figure 2: Comparison of adjacent stimulation-mono measurement pattern (A, B, C) with old pattern (D, E, F), high quality mesh. A and D models with simulated low conductivity (blue circle), B and E calculated conductivity image, C and F calculated resistivity image from noised data

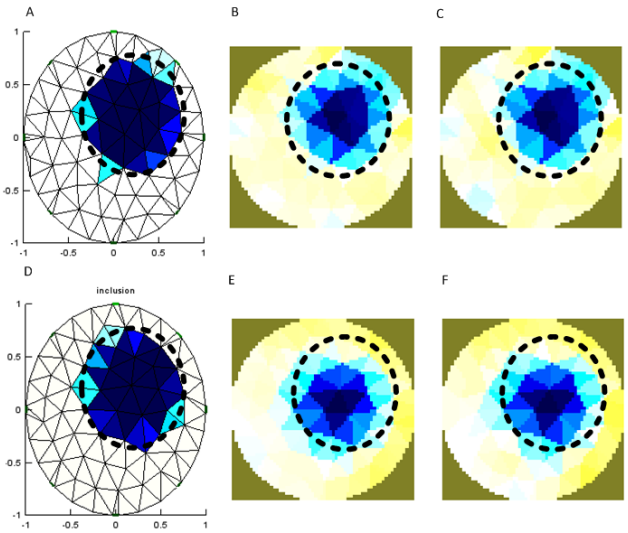

Figure 3: Comparison of adjacent stimulation-mono measurement pattern (A, B, C) with old pattern (D, E, F); low quality mesh. A and D models with simulated low conductivity (blue circle), B and E calculated conductivity image, C and F calculated resistivity image from noised data

noised data have minor reconstruction errors, but at an acceptable level.

4. Experimental setup

After successful validation of the reconstruction algorithm as well as the Matlab model, the operation of the process under the influence of real conditions was studied. This section describes the technical implementation and realization of simultaneous measurement of the resulting voltage differences. In order to acquire this result a vertical flow pipe with a data acquisition system as well as additional components were produced to perform the necessary measurements.

4.1. Tubing of the system

The method was tested in simulations first, then an experimental setup was designed, drawn and fabricated. A 3D model in AutoCAD Inventor was created prior to the manufacture of the individual components and installation of the test setup. An overview of the components is shown below.

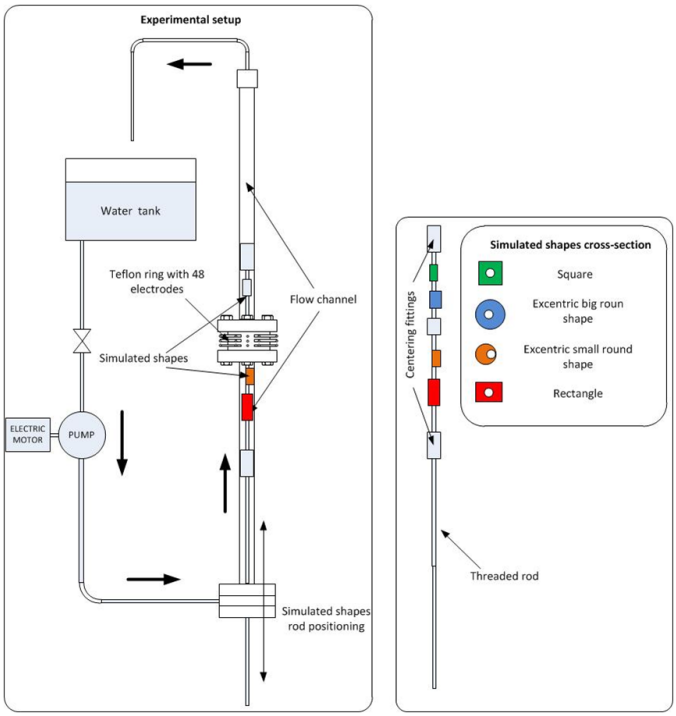

Figure 4: Setup overview

As shown in Fig. 4 the tube which simulates the evaporator tube is a vertical aligned flow channel with inner diameter of 25 mm made from Plexiglas, the middle section consists of flanges. Between the flanges a Teflon ring, also with a 25 mm inner diameter, is mounted which contains 48 stainless steel electrodes arranged in 3 levels with 16 electrodes each. The electrodes are mounted symmetrically and

perpendicular to the flow regime, with an angle of 22.5 degrees between the electrodes. To decrease contact resistance and corrosion, the electrodes were made from a stainless steel round rod of 2 mm diameter. To simulate the lower resistivity inside a pipe, several plastic shapes were made. Those parts were drilled and mounted on a threaded rod to control the position of the rig. Water flow was produced by a centrifugal pump coupled to an electric motor.

4.2. Data Acquisition System

The Installed Data Acquisition System for the real measurements has two main tasks. On one side, the potential at high clock speed must be applied to the various electrodes, on the other side, the same time and the resulting electric voltages are recorded. The implementation of these tasks is explained in detail below.

In the planning and design of the system a very important criterion in the selection of the data acquisition components was the duration of a single measurement and the time required to switch the voltage at the electrodes. As mentioned earlier the implementation of a tomographic measurement series is possible due to applying fast voltage pulses and shuffling the voltage measuring electrodes; fast sampling is important to determine the fluid flowing in an image plane. Therefore, multiplexers are used as distribution components. Channel change takes place in a matter of nanoseconds, which is not possible with mechanical components. Integrated Circuits Logic switches may include an input/output signal and ports to set different channels. For a better understanding of the operation, see the overall system below.

As Fig. 5 shows, tree multiplexers are used: an analog 16-channel multiplexer and demultiplexer type CD4067 by Texas Instruments. The activation of the respective channels via 5 V TTL signals and Boolean algebra. Four terminals on each multiplexer are provided, and a 0 V or 5 V signal can be applied to each, resulting in 2^4 possibilities, resulting in 16 control combinations and thus a specific signal pattern exists for each channel. A fifth port offers the additional possibility of all sixteen channels to lock onto once a 5 V signal is created there; this mode was not

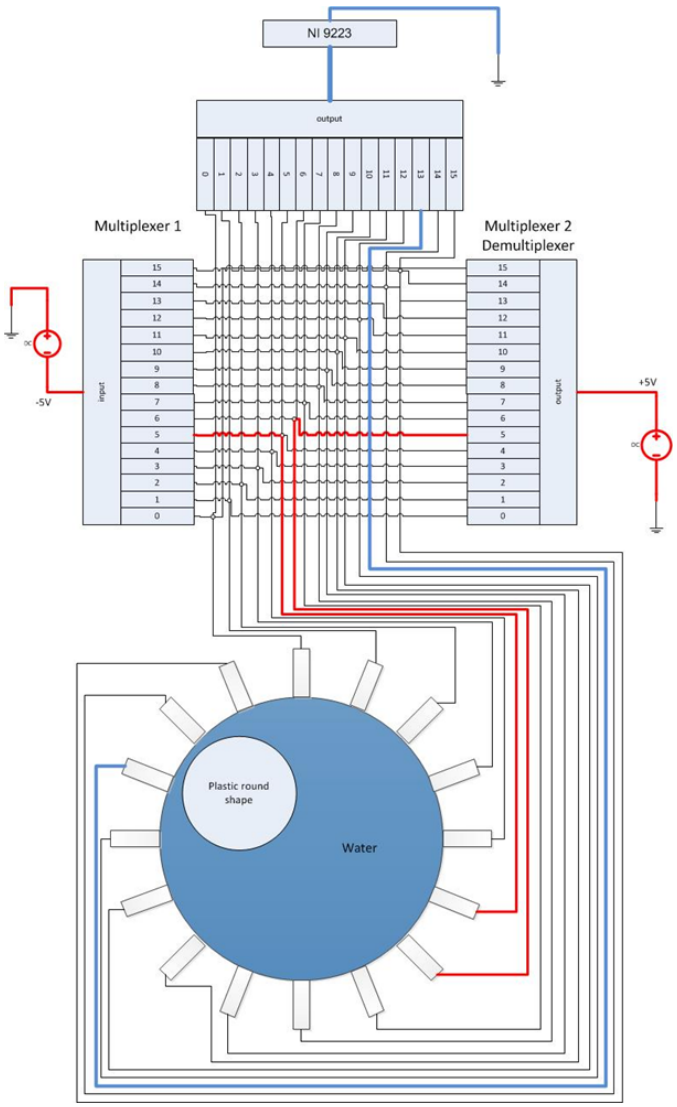

Figure 5: Electrodes switching scheme and current flows in the measurement system

needed so the connection was earthed to the 0 V potential.

Generation of the required signal pattern was done by digital output module NI 9401 from National Instruments, with eight output channels and a clock rate of 10MHz, giving average channel switching of about 100 ns. Configuration and control of this module is performed through a LabView program. Data collection with another module is also implemented via this program

The voltage was measured between multiplexer 3 and the ground block. This shows the phase distribution in cross-section. As a result, the required 256 pairs of electrodes can be automated via the

LabView program and the output module by a suitable sequence of an issued TTL signal pattern. The connection of multiplexers 1 and 2 is synchronous, the connection of multiplexer 3 is also synchronized; since there are eight outputs in the NI9401 module it has sufficient channels to control all multiplexers through the same output module.

Current is generated by two DC constant current sources: one gives potential -2 V, the second +5 V, together giving 7 V of voltage difference between the current supplying electrodes.

To measure the electrical voltage between each electrode and the ground, one analog voltage input module NI 9223 from National Instruments was used. The module has 4 channels (in the experiment only one was used, so the other connection slots were unplugged) and can measure voltages between -10 and +10 V at a scan rate of 1 MS/s per channel. These kinds of modules can only record voltages, and the module is connected between multiplexer 3 and the ground block.

The advantage of the mono-measurement principle (measuring voltage on one electrode), as opposed to measuring voltage between adjacent electrodes, which are connected in series is the bigger voltage difference and therefore thelower noise influence on the measured signal. The very big resistivity of the measuring module, in the range of Giga-Ohms, gives very small charge leakage from pipe volume and good accuracy during measurement.

The measuring module collected data all the time during electrode switching. That gave a huge amount of data (it collects about 100 values of voltage during one electrode combination): since there are 256 electrode combinations there are more than 25600 data points. To obtain a reasonable amount of data, the values are averaged.

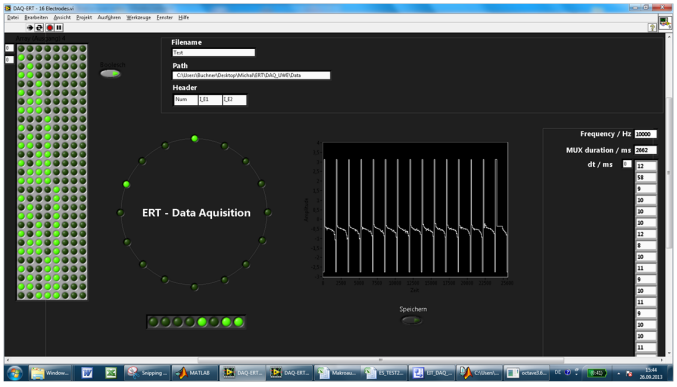

Figure 6: Overview of Labview window. From left: Boolean table for switching electrodes via multiplexers, preview of current connected electrodes, data file path, preview plot of measured voltages, “save” button, additional frequency table

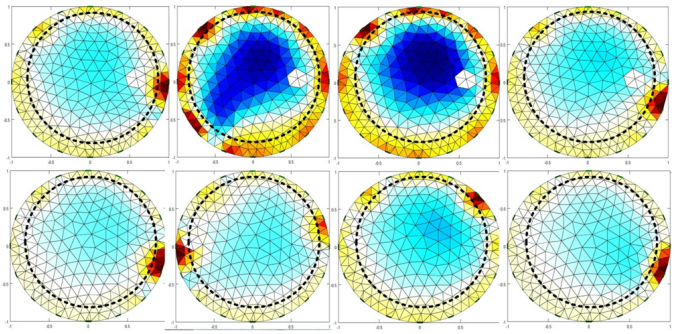

Figure 7: A series of reconstruction of 20 mm diameter circular shape directed to electrode 1

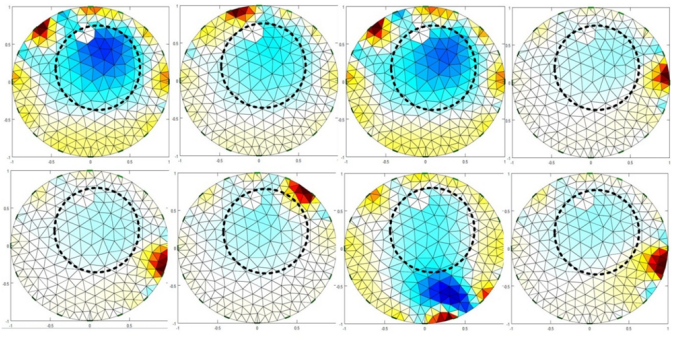

Figure 8: A series of reconstruction of 14 mm diameter cylindrical shape

5. Results

After calibration and frequency adjustments of the measurement system were done, a series of tests were performed with different shapes in different positions. Tests were done in series to gain information about the instability of the measurement system and reconstruction. At the start of the experiment voltages without any shapes were measured inside the flow channel to get homogenous data, because difference solvers were used. Then experiments were

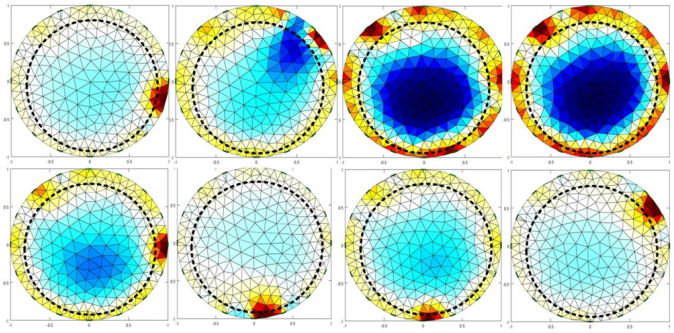

Figure 9: A series of reconstruction of 20 mm diameter cylindrical shape

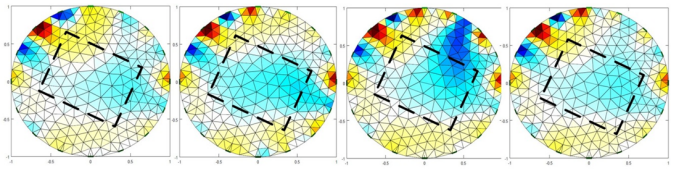

Figure 10: A series of reconstruction of rectangular shape

conducted with specially manufactured shapes: two cylindrical and two rectangular. A few series of reconstructions are shown on Figures 7–10.
Legend:
Blue—low conductivity,
Red—high conductivity,
The dotted line—simulated shape position

6. Discussion

The results are accurate, but contain some errors. High conductivity errors near the electrodes may suggest imperfections in electrode ring manufacturing and electrode placement. The rectangular shape is similar to a circular shape, which results in inaccurate rectangular shape reconstruction.
It is important to have information about changes in the experimental setup. To gain knowledge about instabilities, data with only water in a tube from the beginning of the experiment and after the experiment were collected. Then a difference solver was used in the processing of both data files.

7. Summary and conclusions

The results of the reconstruction were satisfactory. During the development of the two-phase flow EIT sensor several pieces of information were learned.

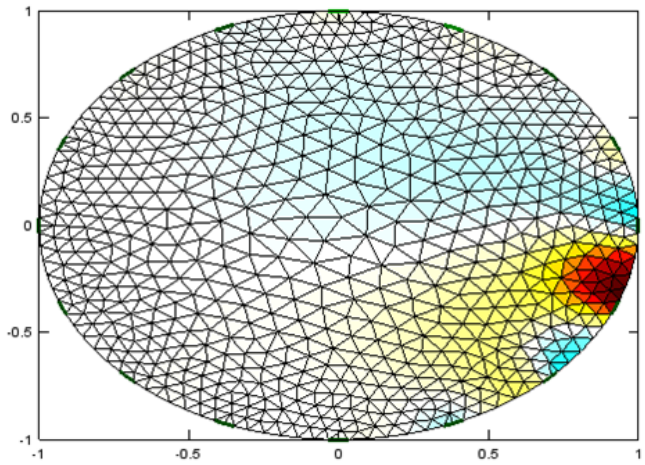

Figure 11: Difference image from data with water at the start of the experiment vs. data with water at the end of the series of experiments

Increasing the number of electrodes can significantly increase the accuracy and spatial resolution of reconstructed images, but a complicated DAQ system and more electrodes heightens the risk of measurement errors, "cold" connections and problems with accurate manufacture. An online working program gives fast and reliable feedback about flow in the vertical flow channel and post-processing codes might be of interest too.
Taking into account the conclusions above, the system presented in this paper should be subject to further testing and development aimed at increasing the accuracy and speed of reconstruction. It is also important to reduce the number and degree of errors. To achieve this, a high-precision electrode ring and electrodes are required.

As shown in Fig. 12 the device is not providing accurate results. To build a real industrial EIT sensor, calibration versus temperature is required.

Acknowledgments

I would like to thank my supervisor Thomas Buchner, promoter Grzegorz Niewiński, head of Areva NP (PTCTT-G), Dr. Schmidt and professors, and my colleagues at Warsaw University of Technology for their continuing encouragement and support.
The publication was created within the framework of a strategic project of the Polish National Center

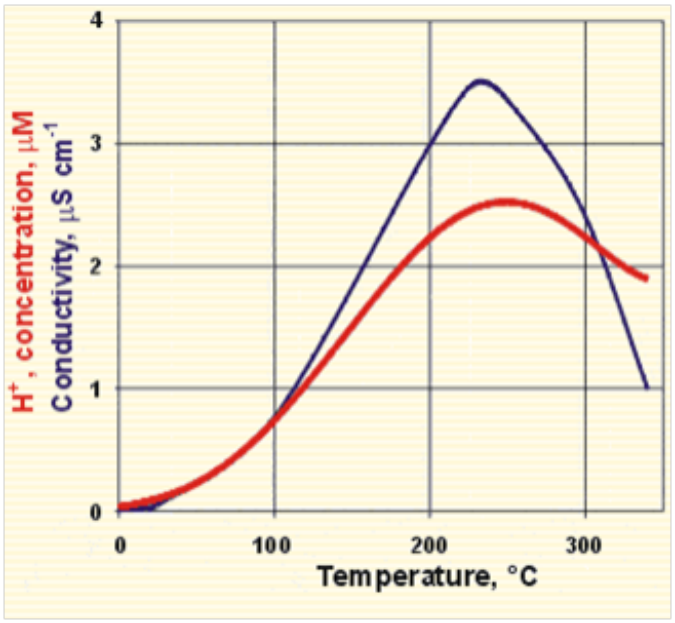

Figure 12: Proton transport in water implies varied water conductivity as a function of temperature [4]

for Research and Development (NCBR): "Technologies for the development of safe nuclear energy", Research Task No. 9 entitled "Development and implementation of safety analysis methods in nuclear reactors during disturbances in heat removal and severe accident conditions".

References

[1] M. Wang, Impedance mapping of particulate multiphase flows, Flow Measurement and Instrumentation 16 (2–3) (2005) 183–189.

[2] N. Polydorides, Image reconstruction algorithms for soft-field tomography, Ph.D. thesis, University of Manchester (2002).

[3] A. Adler, W. R. B. Lionheart, Uses and abuses of eidors: An extensible software base for eit, Physiol. Meas. 27 (2006) 25–42.

[4] J. Han, X. Zhou, H. Liu, Ab initio simulation on the mechanism of proton transport in water, Journal of Power Sources 161 (2) (2006) 1420–1427.